

Comparison of $c(2 \times 2)\text{N}/\text{Fe}(001)$ and $\text{Fe}_4\text{N}(002)$ surfaces: a density-functional theory study

This article has been downloaded from IOPscience. Please scroll down to see the full text article.

2008 J. Phys.: Condens. Matter 20 075212

(<http://iopscience.iop.org/0953-8984/20/7/075212>)

View [the table of contents for this issue](#), or go to the [journal homepage](#) for more

Download details:

IP Address: 129.252.86.83

The article was downloaded on 29/05/2010 at 10:34

Please note that [terms and conditions apply](#).

Comparison of $c(2 \times 2)\text{N}/\text{Fe}(001)$ and $\text{Fe}_4\text{N}(002)$ surfaces: a density-functional theory study

Štěpán Pick¹, Pierre Légaré² and Claude Demangeat³

¹ J Heyrovský Institute of Physical Chemistry of the Academy of Sciences of the Czech Republic, v.v.i., Dolejškova 3, CZ-182 23 Prague 8, Czech Republic

² Laboratoire des Matériaux, Surfaces et Procédés pour la Catalyse, Université Louis Pasteur, ECPM, 25 rue Becquerel, F-67087 Strasbourg Cedex 2, France

³ Institut de Physique et de Chimie des Matériaux de Strasbourg, 23 rue du Loess, F-67034 Strasbourg Cedex 2, France

E-mail: stepan.pick@jh-inst.cas.cz

Received 10 September 2007, in final form 30 November 2007

Published 28 January 2008

Online at stacks.iop.org/JPhysCM/20/075212

Abstract

By using first-principles density-functional theory calculations, we compare the properties of $c(2 \times 2)\text{N}/\text{Fe}(001)$ with the $\text{Fe}_4\text{N}(002)$ surface possessing Fe_2N stoichiometry. We observe a number of similarities as far as the geometry, bond lengths, local density of electronic states and magnetic moments in the surface region are concerned. However, for $c(2 \times 2)\text{N}/\text{Fe}(001)$ the shortest interatomic distance is between N and subsurface Fe atoms, whereas for $\text{Fe}_4\text{N}(002)$ the shortest bond is formed between N and surface Fe atoms, which leads to some important differences. In particular, the magnetic moments are higher for the $c(2 \times 2)\text{N}/\text{Fe}(001)$ surface Fe atoms than for the $\text{Fe}_4\text{N}(002)$ ones, and the opposite is true for the subsurface Fe atoms.

1. Introduction

Among iron nitrides, Fe_4N attracts considerable attention. In metallurgy, the growth of Fe_4N on an iron surface in an N_2 atmosphere represents an important technological process [1, 2]. Because of its magnetic properties, one might think to employ Fe_4N in recording media and magnetic sensors [3, 4]. Moreover, according to reference [5], the coating of ferromagnetic iron microparticles by Fe_4N and Fe_3N improves their stability. In catalysis, the interaction of nitrogen with iron is of the utmost interest as well [6, 7] because of the role of Fe in ammonia synthesis. In experimental studies of the dissociation of N_2 at well-defined Fe surfaces [8–10], an analogy between nitridized iron surfaces and surfaces of Fe_4N has tentatively been suggested. As will be seen in this paper, a simple geometrical explanation for such an analogy exists for (001) surfaces. Actually, two different surfaces with an [001] normal are possible for the nitride. Similarly, as in [10], we reserve the symbol (002) for the nitrogen-containing surface, whereas the pure iron (001) termination, which has not been observed experimentally, is not considered. Together with the unreconstructed $\text{Fe}_4\text{N}(002)$ surface, its more

complex reconstructed modification with excess nitrogen has been prepared [4, 11, 12] and studied theoretically.

Besides the studies mentioned up to now, let us give some references on structural [13] and magnetic [14] measurements of Fe_4N , and also on bulk electronic-structure calculations [15–20]. A theoretical quest into the electronic properties of N on ferromagnetic Fe surfaces was undertaken in [21, 22].

An assessment of possible analogies is of great interest in research, because it might deepen our understanding of similar materials and can offer some new predictive tools. Let us briefly summarize the currently available information. Nonmagnetic electronic and structural properties of $c(2 \times 2)\text{N}/\text{Fe}(001)$ have been studied experimentally [8, 10] and extensive theoretical calculations, including of the surface magnetism, can be found in [22]. The bulk properties of Fe_4N were investigated both by experimentalists and theoreticians in the studies mentioned above. We have also mentioned experimental and theoretical papers devoted to Fe_4N surfaces that concentrate, however, mainly on the reconstructed form. In [4], the spin-averaged density of electronic states (LDOS) for the (002) surface is presented. It is aim of this

Table 1. Work function ϕ and relaxations Δ_{ij} of the vertical iron interlayer distance for the clean and N-covered Fe(001) and Fe₄N(002) surfaces, respectively. The relaxations are calculated with respect to bulk structures. z is the height of adsorbed N above the Fe surface (cf figure 2). d_1 and d_2 are the distances of the surface N to its iron surface and subsurface neighbour, respectively.

| Surface | ϕ (eV) | Δ_{12} (%) | Δ_{23} (%) | Δ_{34} (%) | z (Å) | d_1, d_2 (Å) |
|------------------------|-------------|-------------------|-------------------|-------------------|---------|----------------|
| Fe(001) | 4.06 | -2.26 | 1.66 | 0.04 | | |
| c(2 × 2)N/Fe(001) | 4.35 | 11.88 | -4.60 | 2.69 | 0.30 | 2.04, 1.90 |
| Fe ₄ N(002) | 4.42 | -8.01 | -0.03 | 1.01 | 0.25 | 1.92, 2.00 |

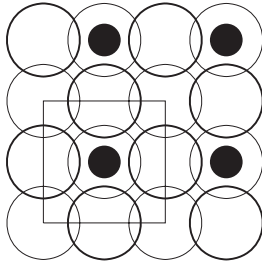


Figure 1. Geometry of the $c(2 \times 2)$ superstructure above the Fe(001) surface or of the γ' -Fe₄N(002) surface (top view). Fe atoms are depicted as open circles and nitrogen atoms positioned in the hollow (4-fold) sites as black dots. Surface (subsurface) Fe atoms are distinguished by thick (thin) lines. The square elementary cell is also shown.

brief paper to compare the (unreconstructed) Fe₄N(002) and $c(2 \times 2)$ N/Fe(001) surfaces by performing first-principles electronic-structure calculations. To the known facts we add a more complete analysis of spin asymmetry at the Fermi level, E_F , for nitrized Fe(001) and evaluate it also for Fe₄N(002). For the latter surface we also offer detailed theoretical data on the geometry, spin-resolved LDOS and magnetic moments on particular surface and subsurface atoms, and a work-function value. Besides this, we perform a comparison of the two strongly similar surfaces and trace some interesting differences and their physical origin.

2. Model and calculation method

The structure of γ' -Fe₄N consists of a face-centred cubic (fcc) iron sublattice with nitrogen positioned in the cube centres. The lattice sites correspond to a *perovskite* lattice but, because of the interchange of transition-metal and anion atoms, respectively, the structure should be denoted [17] as an *antiperovskite* structure. It can also be viewed as a set of parallel Fe₂ and Fe₂N planes alternating in the [001] direction (figure 1). Figure 1 also provides a top view of the Fe₄N(002) surface that we are going to study. Simultaneously, it also represents the geometry of the $c(2 \times 2)$ N/Fe(001) chemisorption system [8, 10, 22] with nitrogen coverage of $\theta = 0.5$. Let us stress that the geometrical similarity between the two surface structures breaks, starting from the third atomic layer (second subsurface layer), and that the nearest-neighbour Fe–Fe distances are about 8% higher in the nitride, as will be described later on.

To perform electronic-structure calculations, the first-principles density-functional theory DACAPO code [23, 24] has been used. It is a plane-wave code utilizing ultrasoft

Vanderbilt pseudopotentials. The lattice constant $a = 3.81$ Å obtained for the bulk Fe₄N correlates rather well with the experimental value of 3.79 Å as well as with other theoretical predictions [13, 16]. This value of lattice constant was used in the Fe₄N(002) surface calculation. A supercell approach using eight-layer slabs (four Fe₂N(002) + four Fe₂(001) layers) alternating with vacuum layers about 14 Å wide was employed. The upper surface of the slab has Fe₂N character, and atoms in the four upper layers are allowed to relax. Due to the relaxation, the planes become buckled. The energy cutoff for plane waves is equal to 400 eV. A correcting dipole field is applied to compensate for possible electrostatic interaction between slabs, and a Monkhorst–Pack ($8 \times 8 \times 1$) sampling of the Brillouin zone is used. The exchange–correlation energy functional was chosen in the gradient-corrected Perdew–Wang (PW91) [25] form. The data for the bulk body-centred cubic (bcc) Fe, Fe(001) slab and for the $c(2 \times 2)$ N/Fe(001) chemisorption system (including some unpublished data on spin asymmetry) are mostly taken from [22]. The details of the calculation employed in [22] are very similar to those used for Fe₄N(002) here. The local magnetic moments and local density of electronic states are related to spheres with the (bulk) Wigner–Seitz radius of 1.41 Å for Fe atom in the iron crystal and 1.48 Å in the nitride. For nitrogen, the covalent radius 0.7 Å [22] proposed in the literature was chosen.

3. Results and discussion

Before presenting the results of surface calculations, it is useful to mention some experimental data on interatomic distances in the bulk. The Fe–N separation in Fe₄N is 1.90 Å. The Fe–Fe nearest-neighbour distance is 2.48 Å for bcc α -iron, and 2.68 Å for γ' -Fe₄N. (In the calculation [22], a bcc iron lattice constant of $a = 2.855$ Å was obtained, which is slightly lower than the experimental value of 2.87 Å.) For the high-temperature phase of fcc γ iron, the Fe–Fe distance is 2.59 Å as a result of thermal effects. It is only 2.43 Å in the hypothetical paramagnetic γ -iron, which is, however, unstable [26] with respect to further deformations. In tables 1–3, we also provide some calculated data on the clean Fe(001) surface, and on the bulk properties of bcc Fe and Fe₄N, respectively. The bulk data are based on three-dimensional (not slab) structure calculations.

3.1. The $c(2 \times 2)$ N/Fe(001) surface

The electronic work function and structural parameters of (001) surfaces are displayed in table 1; see also figure 2. As usual, the interplanar relaxation (as a percentage) is defined as $\Delta_{ij} = 100(d_{ij} - d)/d$, where d_{ij} is the Fe interplanar

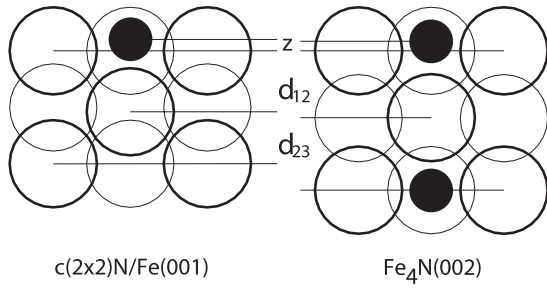


Figure 2. Side view of the relaxed geometry (surface + two subsurface planes) at the Fe(001) surface with adsorbed nitrogen, and at the γ' -Fe₄N(002) surface. Fe atoms are depicted as open circles, and nitrogen atoms as black dots. Iron atoms that lie (do not lie) in the same vertical plane as nitrogen are distinguished by thick (thin) lines. Definitions of the vertical N–Fe (surface) separation z and the vertical separations of the iron layers, d_{12} and d_{23} , are shown. The first iron layers in the two systems are aligned in the figure.

Table 2. Magnetic moments (in μ_B) calculated for the surface nitrogen (N), iron or nitrogen of the first three iron layers (Fe₁–Fe₃, N₃) and in the bulk (Fe_b, N_b). In the second layer and in the bulk, nonequivalent Fe atoms can exist; in such a case, the moment value at Fe that is closer to N is given first.

| Layer | Fe(001) | c(2 × 2)N/Fe(001) | Fe ₄ N(002) |
|-----------------|---------|-------------------|------------------------|
| N | | −0.06 | −0.01 |
| Fe ₁ | 3.05 | 2.71 | 2.47 |
| Fe ₂ | 2.38 | 1.84, 2.61 | 2.19, 2.95 |
| Fe ₃ | 2.35 | 2.42 | 2.29 |
| N ₃ | | | 0.00 |
| Fe _b | 2.29 | | 2.29, 3.01 |
| N _b | | | 0.02 |

separation between neighbouring planes i and $j = i + 1$, and d is the ideal (bulk) interlayer spacing. (Because of the buckling of layers, we always choose the layer level defined by the Fe atom that is closest to the surface nitrogen atom.) We can compare [22] the results of calculations for c(2 × 2)N/Fe(001) (table 1) with experimental data [8, 10]. The measured rise of the work function after nitrogen adsorption by 0.33 ± 0.02 eV compares favourably with the calculated value of 0.29 eV. Similarly, the N–Fe(surface) distance of 2.04 Å is in good agreement with the measured value of 2.04 ± 0.05 Å. The change in the work function correlates with the expected charge polarization introduced by electronegative adsorbates [21]. For the N–Fe(subsurface) the bond length is shorter; the LEED experiment [10] claims a slightly shorter value (1.83 Å) than our finding 1.90 Å. We get a buckling of about 0.1 Å in the subsurface Fe layer—an effect which is not analysed in [10]. Because of the large surface expansion (table 1), the Fe(surface)–Fe(subsurface) distances are 2.62 Å (for the Fe atom vertically below N) and 2.51 Å. The short N–Fe(subsurface) bond length points to a strong interaction which is manifested by the presence of a very deep dip at the Fermi level (figure 3) of the spin-resolved local density of electronic states found for the minority-spin states at subsurface iron atoms. For the surface Fe atom, E_F falls into a peak in the minority-spin LDOS. This might indicate that the N–Fe(subsurface) bond is stronger than the N–Fe(surface)

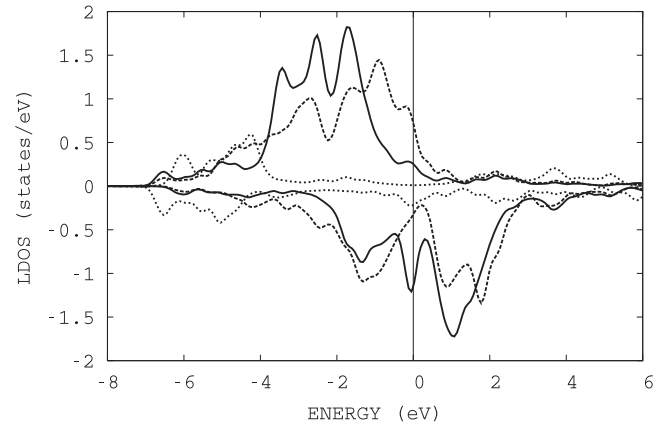


Figure 3. Spin-resolved local densities of electronic states (LDOS) for the c(2 × 2)N/Fe(001) system. Spin \uparrow states are displayed in the upper half of the figure, and spin \downarrow (negative LDOS) states in the lower part of the figure. Note that spin \uparrow states are the majority-spin states for Fe and minority-spin states for N. Full and dashed lines correspond to the d-electron LDOS at surface or subsurface iron atoms, respectively. The dotted lines mark s, p-electron nitrogen states. The Fermi level coincides with the energy zero. From [22].

bond, as is also suggested by the bond lengths 1.90 Å versus 2.04 Å (table 1).

Let us now consider the magnetization of particular atoms. For bulk α -Fe we get (table 2) a slightly higher magnetic moment of 2.29 μ_B than the experimental value of 2.22 μ_B . For the Fe(001) surface we find a marked magnetization enhancement caused mainly by the reduced coordination of surface atoms. The surface magnetization is lowered by nitrogen adsorption. The most marked reduction, however, takes place for the iron atom lying just below the N adatom, which apparently correlates with the shorter distance and strong Fe–N interaction described above. These results show that the Fe–N interaction effect outweighs the surface-expansion effect which ‘itself’ should lead to magnetization promotion. For another nonequivalent subsurface Fe atom that is more distant from N, one finds a higher magnetization than for clean Fe(001) (table 2). It is difficult to decide whether this is due to a small Fe–Fe separation increase (2.51 Å) or whether it is rather a result of magnetization oscillation common in nonhomogeneous structures. Above the (001) surface, we find antiferromagnetic N–Fe coupling (table 2) with a small magnetic moment induced on N. We shall return to this point in the next subsection.

A useful quantity, which can also be studied experimentally [27], is the spin asymmetry (or spin-polarization ratio [3]) $A = (\rho_{\uparrow} - \rho_{\downarrow})/(\rho_{\uparrow} + \rho_{\downarrow})$, where ρ_{\uparrow} , ρ_{\downarrow} stand for the iron majority- or minority-spin LDOS at a chosen energy (the definition differing by a minus sign can also be found in the literature). Having in mind both the bonding properties and possible kinetic effects [3], we shall consider the LDOS at the Fermi level E_F . Since mainly d-electrons are responsible for the spin polarization, the spin asymmetry A_d based on the d-electron LDOS only will also be considered (table 3). It is seen that A_d is always higher (in absolute value) than A , but the trends are the same for A and A_d , respectively. For the clean Fe(001)

Table 3. Spin asymmetry A at the Fermi level calculated for iron atoms in the first two layers (Fe_1 , Fe_2) and in the bulk (Fe_b). For A_d , only d-electrons are taken into account. When nonequivalent Fe atoms exist, the first value refers to the atom closer to N and the third value is the mean value of the asymmetry.

| System | Fe_1 | Fe_2 | Fe_b |
|--|---------------|------------------------|------------------------|
| $\text{Fe}(001)$, A | -0.895 | -0.481 | -0.405 |
| $\text{Fe}(001)$, A_d | -0.955 | -0.491 | -0.422 |
| $c(2 \times 2)\text{N}/\text{Fe}(001)$, A | -0.566 | 0.381, -0.347; 0.148 | |
| $c(2 \times 2)\text{N}/\text{Fe}(001)$, A_d | -0.635 | 0.381, -0.373; 0.156 | |
| $\text{Fe}_4\text{N}(002)$, A | -0.360 | -0.422, -0.814; -0.575 | -0.595, -0.868; -0.650 |
| $\text{Fe}_4\text{N}(002)$, A_d | -0.409 | -0.464, -0.880; -0.623 | -0.652, -0.926; -0.707 |

surface, A is almost -1 , and it is more than twice as large as the bulk value. For iron at the $c(2 \times 2)\text{N}/\text{Fe}(001)$ surface, the asymmetry enhancement is not so large, and for the subsurface iron atoms placed just below nitrogen the asymmetry even changes sign. This is, of course, a result of the presence of the dip in the minority-spin LDOS (figure 3) discussed above.

3.2. The $\text{Fe}_4\text{N}(002)$ surface

Table 1 shows that nitrogen atoms move above the iron layer when the surface is formed. It is clear from figure 2 that the relaxed geometry is quite similar to that of nitridized $\text{Fe}(001)$. According to the same table, the two work-function values are similar as well. Also, the Fe–N distances become quite analogous, with an interesting qualification: the distances of N from surface and subsurface iron atoms, respectively, can be viewed as approximately interchanged when we compare $c(2 \times 2)\text{N}/\text{Fe}(001)$ and $\text{Fe}_4\text{N}(002)$ surfaces. We shall show later that, as a result, some surface and subsurface electronic and magnetic properties become interchanged as well. The surface iron layer is *relaxed* for $\text{Fe}_4\text{N}(002)$, which leads to surface–subsurface Fe bond shortening: 2.59 and 2.60 Å. These values resemble the distance of 2.62 Å quoted in section 3.1. The buckling of the subsurface iron layer (~ 0.01 Å) is small.

The surface LDOS were presented in [4] where, however, they were averaged over the two spin orientations. In figure 4 we display more detailed information. Although the gross features in figures 3 and 4 are alike, important differences near E_F are seen. There is a dip (figure 4) for minority-spin states that is comparable for surface and subsurface Fe atoms at E_F . For the surface Fe atom LDOS, the Fermi level falls well inside this dip for $\text{Fe}_4\text{N}(002)$. The dip is much less marked, however, than the dip for the subsurface Fe atom in figure 3. Hence, a comparison of bond lengths might point to a somewhat stronger interaction of nitrogen with surface Fe atoms than with subsurface atoms in $\text{Fe}_4\text{N}(002)$. The large majority-spin LDOS peak for subsurface Fe in figure 4 corresponds to the feature found experimentally and theoretically 1.4 eV below E_F in [4].

Starting from calculated properties of (bulk) iron nitrides, Matar concluded [17] that the interaction of iron with nitrogen leads to magnetization suppression compared with analogous pure Fe structures, the magnitude being sensitive to the nitrogen concentration and to atomic-volume variation. If, however, the atomic volume of a Fe atom is large enough, its magnetic moment attains a saturation value of about $3 \mu_B$ that is only slightly sensitive to geometrical details. These

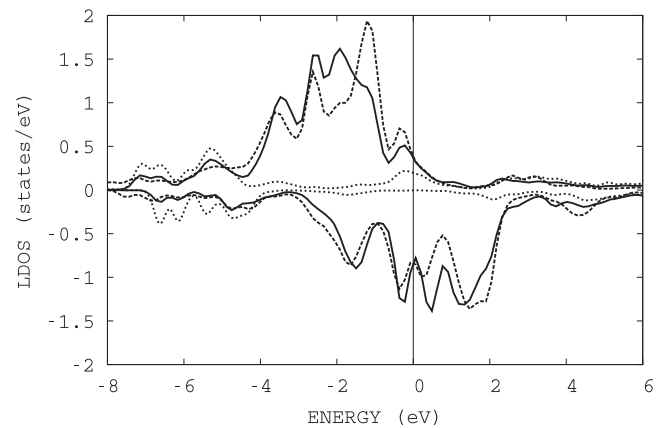


Figure 4. Spin-resolved local densities of electronic states (LDOS) for the $\text{Fe}_4\text{N}(002)$ system. Spin \uparrow states are displayed in the upper half of the figure, and spin \downarrow (negative LDOS) states in the lower part of the figure. Note that spin \uparrow states are the majority-spin states for Fe and minority-spin states for surface N. Full and dashed lines correspond to the d-electron LDOS at surface or subsurface iron atoms, respectively. The dotted lines mark s, p-electron nitrogen states. The Fermi level coincides with the energy zero.

trends are well documented for the bulk Fe_4N and also remain valid near the (002) surface. Naturally, an analogous magnetization reduction was also encountered in the previous subsection. In the γ' - Fe_4N crystal, two nonequivalent Fe atoms are present. There is agreement in the literature that the moment of an Fe atom more distant from N (Fe(I)) is close to $3 \mu_B$. For the second iron atom (Fe(II)), there is some scatter in the literature data [4, 14–20] and values closer to $2 \mu_B$ than our finding $2.29 \mu_B$ in table 2 can be found. Let us note that our conclusions on the magnetic moments of particular bulk atoms correlate quite well with recent calculations [20]. For $\text{Fe}_4\text{N}(002)$, the surface (subsurface) iron magnetization is lower (higher) than for the $c(2 \times 2)\text{N}/\text{Fe}(001)$ system. The difference might be related to the ‘interchanged’ length of surface and subsurface Fe–N bonds. Several authors [21, 22, 28–32] observed, for some chemisorption systems, antiferromagnetic adsorbate–surface coupling with a small magnetic moment induced on adsorbates. In [31], an attempt to relate this effect to a strong covalent bond was undertaken. Here, we obtain a small magnetic moment on nitrogen in the Fe_4N bulk that couples *ferromagnetically* to iron (a very small *negative* moment is predicted in the linear muffin-tin orbital (LMTO) calculation of [15]), and practically no magnetization of N in the subsurface region. For both

$c(2 \times 2)\text{N}/\text{Fe}(001)$ and $\text{Fe}_4\text{N}(002)$ surfaces, however, we predict *antiferromagnetic* N–Fe coupling (table 2).

The spin asymmetry in the bulk Fe_4N (table 3) of $A = -0.65$ agrees well with the value of -0.6 in [3]. When we move towards the surface, the asymmetry is lowered for the subsurface, and especially for surface iron atoms.

4. Conclusions

In this paper we have compared two specific nitrogen-covered surfaces: a nitrogen overlayer with coverage of $\theta = 0.5$ on bcc $\text{Fe}(001)$, and a surface of nitride $\text{Fe}_4\text{N}(002)$. Clear similarities between the $c(2 \times 2)\text{N}/\text{Fe}(001)$ and the surface of $\text{Fe}_4\text{N}(002)$ were depicted but, on closer inspection, important differences were also discovered that correlate with differing N–Fe distances. In particular, the interlayer distances at surfaces are modified for both systems, which allows us to achieve appropriate interatomic distances. The Fe–Fe separation between a surface iron atom and a subsurface atom in interaction with N (an Fe atom below N) lies well between the corresponding bulk α -Fe and γ' - Fe_4N values. However, two kinds of Fe–N bonds are formed: a short one with a length close to the separation 1.9 \AA in the bulk Fe_4N , and another one that is longer ($\sim 2 \text{ \AA}$). These bonds are ‘interchanged’ for the two surfaces: short bonds between N and subsurface iron are formed at $\text{Fe}(001)$, whereas for $\text{Fe}_4\text{N}(002)$ they take place between N and surface Fe atoms. It is mainly the short bond that influences the local electronic and magnetic properties. As a result, the local density of electronic states, magnetic moment and spin asymmetry at the Fermi level vary more unevenly in the sequence surface–subsurface–bulk for $c(2 \times 2)\text{N}/\text{Fe}(001)$, where even the sign of the spin asymmetry alternates. For surface nitrogen, we get a very small magnetic moment that couples antiferromagnetically to the iron atom moments. Its value is, however, negligible for $\text{Fe}_4\text{N}(002)$.

Acknowledgment

ŠP is indebted to Université Louis Pasteur, Strasbourg, for kind hospitality and financial support.

References

- [1] Fast J D 1965 *Interaction of Metals and Gases* vol 1 (Eindhoven: Philips Technical Library) especially sec. 7.8
- [2] Appolaire B and Gouné M 2006 *Comput. Mater. Sci.* **38** 126
- [3] Kokado S, Fujima N, Harigaya K, Shimizu H and Sakuma A 2006 *Phys. Rev. B* **73** 172410
- [4] Navio C, Alvarez J, Capitan M J, Ecija D, Gallego J M, Ynduráin F and Miranda R 2007 *Phys. Rev. B* **75** 125422 and references therein
- [5] Luo X and Liu S 2007 *J. Magn. Magn. Mater.* **308** L1
- [6] Lundqvist B I 1983 *Vacuum* **33** 639
- [7] Dahl S, Logadottir A, Jacobsen C J H and Nørskov J K 2001 *Appl. Catal. A* **222** 19 and references therein
- [8] Bozso F, Ertl G, Grunze M and Weiss M 1977 *J. Catal.* **49** 18
- [9] Bozso F, Ertl G and Weiss M 1977 *J. Catal.* **50** 519
- [10] Imbihl R, Behm R J, Ertl G and Moritz W 1982 *Surf. Sci.* **123** 129
- [11] Gallego J M, Boerma D O, Miranda R and Ynduráin F 2005 *Phys. Rev. Lett.* **95** 136102
- [12] Ecija D, Jimenez E, Camarero J, Gallego J M, Vogel J, Mikuszeit N, Sacristián N and Miranda R 2007 *J. Magn. Mater.* **316** 321
- [13] Jacobs H, Rechenbach D R and Zachwieja U 1995 *J. Alloys Compounds* **227** 10
- [14] Frazer B C 1958 *Phys. Rev.* **112** 751
- [15] Sakuma A 1991 *J. Magn. Magn. Mater.* **102** 127
- [16] Timoshevskii A N, Timoshevskii V A and Yanchitski B Z 2001 *J. Phys.: Condens. Matter* **13** 1051
- [17] Matar S F 2002 *C. R. Chimie* **5** 539
- [18] Matar S F 2002 *J. Alloys Compounds* **345** 72
- [19] Ogura M and Akai H 2004 *Hyperfine Interact.* **158** 19
- [20] Zhao E, Xiang H, Meng J and Wu Z 2007 *Chem. Phys. Lett.* **449** 96
- [21] Jenkins S J 2006 *Surf. Sci.* **600** 1431
- [22] Pick Š, Légaré P and Demangeat C 2007 *Phys. Rev. B* **75** 195446
- [23] *Ab initio* pseudopotential code DACAPO developed at CAMPOS (Center for Atomic-Scale Materials Physics) Dept. of Physics, Technical University of Denmark, Lyngby see <https://wiki.fysik.dtu.dk/dacapo>
- [24] Hammer B, Hansen L B and Nørskov J K 1999 *Phys. Rev. B* **59** 7413
- [25] Perdew J P, Chevary J A, Vosko S H, Jackson K A, Pederson M R, Singh D J and Fiolhais C 1992 *Phys. Rev. B* **46** 6671
- [26] Marcus P M, Moruzzi V L and Qiu S-L 1999 *Phys. Rev. B* **60** 369
- [27] Sun X, Förster S, Li Q X, Kurahashi M, Suzuki T, Zhang J W, Yamauchi Y, Baum G and Steidl H 2007 *Phys. Rev. B* **75** 035419
- [28] Pick Š and Dreyssé H 2000 *Surf. Sci.* **460** 153
- [29] Geng W T, Freeman A J and Wu R Q 2001 *Phys. Rev. B* **63** 064427
- [30] Pick Š and Dreyssé H 2001 *Surf. Sci.* **474** 70
- [31] Pick Š and Dreyssé H 2003 *Surf. Sci.* **540** 389
- [32] Sorescu D C 2006 *Phys. Rev. B* **73** 155420